Stalagmite from the Austrian Alps reveals Dansgaard–Oeschger events during isotope stage 3: Implications for the absolute chronology of Greenland ice cores

Christoph Spötl [a,*], Augusto Mangini [b]

[a] *Institut für Geologie und Paläontologie, Universität Innsbruck, Innrain 52, 6020 Innsbruck, Austria*
[b] *Forschungsstelle Radiometrie, Heidelberger Akademie der Wissenschaften, Im Neuenheimer Feld 229, 69120 Heidelberg, Germany*

Abstract

A mass-spectrometric uranium-series dated stalagmite from the Central Alps of Austria provides unprecedented new insights into high-altitude climate change during the peak of isotope stage 3. The stalagmite formed continuously between 57 and 46 kyr before present. A series of 'Hendy tests' demonstrates that the outer parts of the sample show a progressive increase of both stable C and O isotope values. No such covariant increase was detected within the axial zone. This in conjunction with other observations suggests that the continuous stable oxygen isotope profile obtained from the axial zone of the stalagmite largely reflects the unaltered isotopic composition of the cave drip water. The $\delta^{18}O$ record shows events of high $\delta^{18}O$ values that correlate remarkably with Interstadials 15 (a and b), 14 and 12 identified in the Greenland ice cores. Interstadial 15b started rapidly at 55.6 kyr and lasted $\sim$300 yr only, Interstadial 15a peaked 54.9 kyr ago and was even of shorter duration ($\sim$100 yr), and Interstadial 14 commenced 54.2 kyr ago and lasted $\sim$3000 yr. This stalagmite thus represents one of the first terrestrial archives outside the high latitudes which record precisely dated Dansgaard–Oeschger (D/O) events during isotope stage 3. Provided that rapid D/O warmings occurred synchronously in Greenland and the European Alps, the new data provide an independent tool to improve the GRIP and GISP2 chronologies.
© 2002 Elsevier Science B.V. All rights reserved.

Keywords: speleothemS; Th/U dating; Pleistocene; Alps; Austria

1. Introduction

The recognition of an inherently unstable climate during the Late Quaternary represents a milestone in paleoclimatology. The large, abrupt changes during the last glacial period came as a big surprise when first reported from the Greenland Ice Core Project (GRIP) [1,2]. Subsequently referred to as Dansgaard–Oeschger (D/O) events, these high-frequency fluctuations are manifested in the ice cores as rapid increases in the stable hydrogen and oxygen isotopic compositions, relatively short peak warm conditions, followed by a

---

* Corresponding author. Tel.: +43-512-507-5593;
Fax: +43-512-507-2914.
E-mail address: christoph.spoetl@uibk.ac.at (C. Spötl).

gradual decrease of the stable isotopic values toward cold (stadial) conditions. The amplitudes and rates of these swings in air temperature over central Greenland were substantial and reached up to 16°C over a few decades [3,4].

D/O-induced climate change is centered on the North Atlantic and on regions with strong atmospheric response to changes in that area [5,6,7,8]. Millennial-scale fluctuations in sea-surface temperatures [9,10] and upwelling intensity [11] with striking similarities to the Greenland Interstadials (GIS) are, however, also reported from other oceanic sites. Most importantly, variations of the methane content of ice in both Greenland and Antarctica parallel Greenland warmings [12], thus providing strong evidence that the Earth as a whole experienced this unstable climatic rhythm during glacial times.

The generally westerly atmospheric circulation over Europe makes it very likely that the equivalents of the Greenland D/O events also existed in Europe. Yet, continental records showing supporting evidence are rare, commonly incomplete and compromised by imprecise dating. Recently, high-frequency climate variability has been inferred from long pollen records in the Mediterranean region and tentatively correlated with D/O events from Greenland ice cores [13,14,15]. Unambiguous peak-to-peak correlation, however, is still hampered by dating problems of both lacustrine successions and ice cores. The latter chronologies involve significant dating uncertainties of up to ± 5 to ± 10% during isotope stages 3 [16], which are large in comparison to the high-frequency variability during this time interval.

Here we present a continuous segment of 11-kyr speleothem calcite deposition from a high-altitude cave in the Eastern Alps of Austria during isotope stage 3 which clearly shows D/O climate dynamics. In contrast to other terrestrial records, this new record is precisely dated using Th/U, thus providing the rare opportunity to date D/O events and to compare them with the existing ice core chronologies.

1.1. Study site

Kleegruben Cave (Austrian Cave Inventory no. 2411/14) is located in the western part of the Zillertal Alps of Tyrol (Fig. 1). Similar to the nearby extensive Spannagel Cave [17], this cave developed in Jurassic calcite marble tectonically sandwiched between gneiss. The entrance to Kleegruben Cave is located at approximately 2165 m a.s.l. above a ∼20-m high cliff, which forms the eastern margin of the broad SSE–NNW trending Sandeck ridge separating two glaciers further south (Fig. 1). During the Little Ice Age (LIA) both glaciers advanced considerably to the north. The eastern glacier stopped some 800–900 m south of Kleegruben Cave, whereas the significantly larger Hintertux Glacier went further north and deposited a sharp-crested lateral moraine ridge along the western margin of the Sandeck ridge (Fig. 1). Both glaciers apparently coalesced across the northern part of the ridge during the Late Glacial as indicated by the presence of two segments of a broad and vegetated moraine ridge (Fig. 1). The ubiquitous presence of allochthonous gneiss cobbles and unconsolidated sand-size sediments in Kleegruben Cave demonstrates that meltwater of the Würm glacier entered the cave during the Last Glacial Maximum (and possibly also during the Late Glacial). Speleothems are rare in Kleegruben Cave which is not surprising considering that the interior cave air temperature is only +2.3°C (measured using data logger over a period of 1.5 yr). Modern calcite deposition only occurs as soda straws and rare helictites.

Stalagmite sample SPA 49, located 40 m from the cave entrance, was inactive at the time of sampling and apparently survived erosion by glaciofluvial meltwater only because it formed at an elevated position below the ceiling of a larger chamber.

2. Methods

The sample was cut parallel to the growth axis using a diamond saw and the central segment was examined in polished slabs and petrographic thin sections. Samples for stable oxygen isotope analysis were drilled along the central axis of the stalagmite using a 0.5-mm drill bit (1-mm intervals). In addition, we attempted to sample along indi-
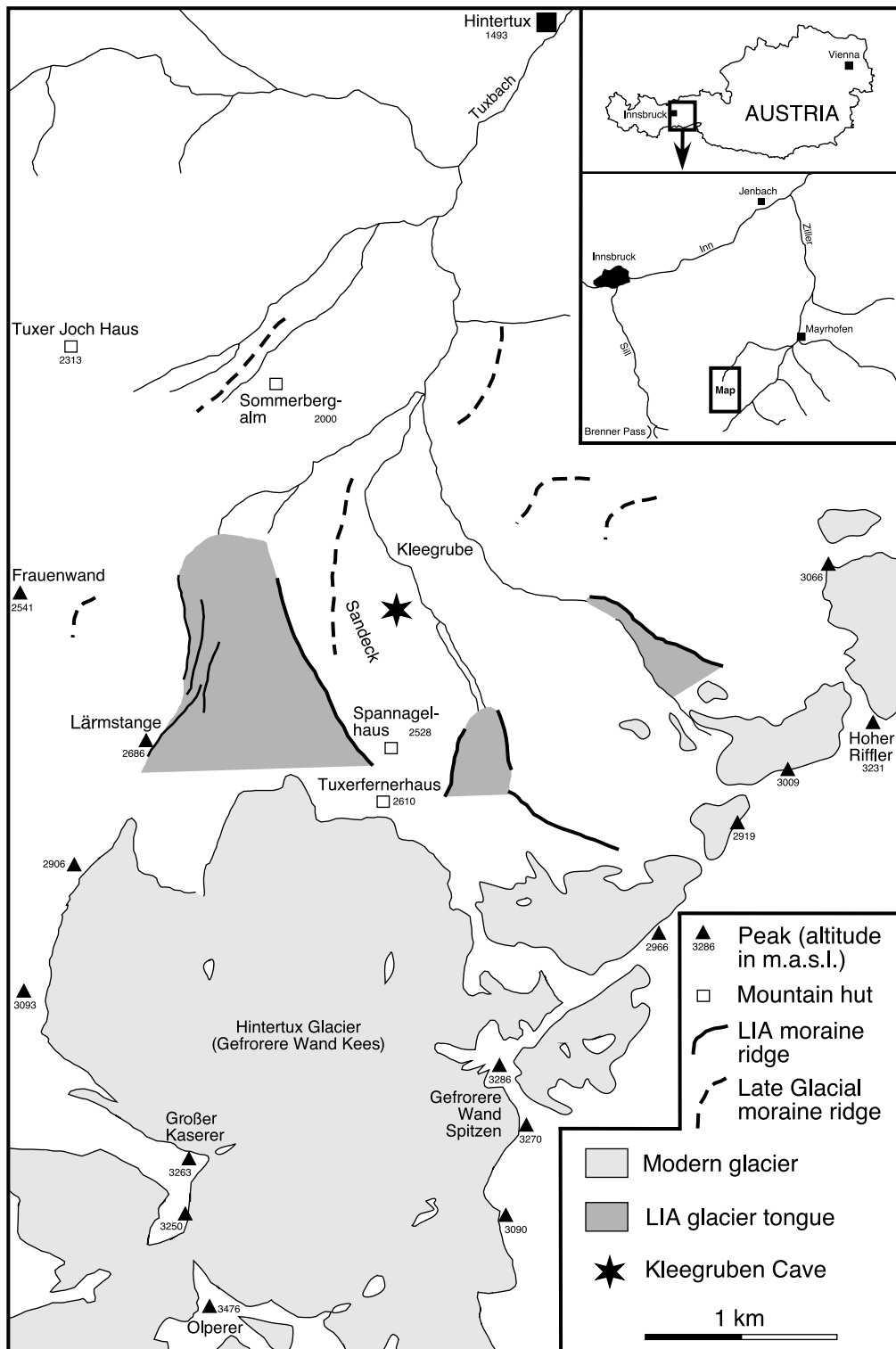
Fig. 1. Location of the study site (Kleegruben Cave; 47.0882°N, 11.6715°E). Abbreviation: LIA, Little Ice Age.

vidual growth layers from the axis laterally down the flank at nine different levels within the stalagmite. Given the poor development of laminae in this speleothem, precise location of the drill was ambiguous in some cases. The stable C and O isotope composition was measured on a DeltaplusXL mass spectrometer equipped with an automated carbonate preparation system (Gasbench II). Results are reported relative to the Vienna PeeDee Belemnite standard and standardization was accomplished using NBS 19. Precision of $\delta^{18}O$ values expressed as the 1-sigma standard deviation is smaller than 0.10‰.

Fifteen samples taken along the extension axis were dated using the ^{230}Th–^{234}U disequilibrium method. Th/U measurements were performed on a MAT 262 RPQ mass spectrometer with a double filament technique. Half lives of ^{238}U, ^{234}U and ^{230}Th are based on [18]. For analytical details see [19]. Ages were corrected for initial detrital ^{230}Th under the assumption of an activity ratio of $^{230}Th/^{232}Th$ like average crust. The correction comes up to less than 50 yr, except for one sample (at 0.5 cm; Table 1) with a value of 460 yr.

2.1. Sample description

SPA 49 is a 29.5-cm high, slightly conical sta-lagmite composed of dense, whitish columnar low-Mg calcite, the outer surface of which is coated by a medium-gray calcite layer less than 1 mm thin (Fig. 2). The topmost 8 mm are gray colored and show a couple of thin layers with higher amounts of impurities. The remainder of the sample shows sub-mm layering that is thicker but less distinct in the axial zone than on the outer flanks. There is neither macroscopic nor microscopic evidence of unconformities within the stalagmite.

3. Results

The calcite of SPA 49 is rich in U, ranging from 9.47 to 74.95 ppm. $^{230}Th/^{232}Th$ activity ratios are high (above 5700) indicating that detrital Th is negligible. The only exception is the topmost sample which yielded a lower ratio of 67, consistent with its light-gray color. The resultant ages are in stratigraphic order and range from 57.38 ± 0.54 to 47.48 ± 0.51 kyr (Table 1; Fig. 3). An age model based on a 6th order polynom is used here to fit the data with an R of 0.998. A two-step linear age model yields a slightly lower R of 0.991 for the time interval 57.4–50.4 kyr (Fig. 3). Both age models suggest a near-linear accretion rate of

Table 1
Th/U ages.

Lab. No.	Distance from top	$\delta^{234}U$		Conc. ^{238}U		Conc. ^{232}Th		Conc. ^{230}Th		Age	
	(cm)	(‰)	±(‰)	(μg/g)	±(μg/g)	(ng/g)	±(ng/g)	(pg/g)	±(pg/g)	(kyr)	±(kyr)
2080	0.5	23.8	3.7	9.467	0.019	155.48	0.84	56.44	0.42	47.48	0.51
2702	1.7	14.3	2.5	18.169	0.027	3.096	0.022	109.07	0.87	48.95	0.52
2131	3.0	21.7	3.2	28.582	0.057	5.738	0.026	177	1.1	50.44	0.45
2503	6.0	17.1	1.7	34.973	0.035	6.704	0.016	217.04	0.76	50.87	0.26
2569	6.5	14.4	2.1	36.195	0.040	3.866	0.010	224.41	0.67	50.99	0.24
2703	9.4	14.7	1.4	41.682	0.042	2.5778	0.0059	261.5	0.65	51.74	0.20
2504	12.0	11.0	3.1	46.083	0.074	1.589	0.011	290.4	2.3	52.30	0.57
2704	14.4	11.2	1.6	58.948	0.065	8.12	0.019	379.4	1.1	53.71	0.24
2292	16.0	9.3	1.7	41.687	0.050	2.0735	0.0093	269.2	1.1	54.11	0.32
2506	16.0	11.2	1.9	39.787	0.056	4.253	0.015	256	1.5	53.70	0.44
2505	17.0	5.4	1.9	56.311	0.062	1.278	0.010	365.2	3.7	54.70	0.72
2705	20.0	10.4	1.4	74.954	0.075	2.7099	0.0054	490.5	1.0	54.96	0.18
2290	23.0	10.0	2.1	61.349	0.092	0.7281	0.0033	404.3	1.8	55.49	0.38
2507	26.0	8.0	1.9	56.098	0.067	2.964	0.011	373.9	1.9	56.48	0.42
1911	29.0	10.5	3.4	40.398	0.097	2.311	0.012	273.3	1.6	57.38	0.54

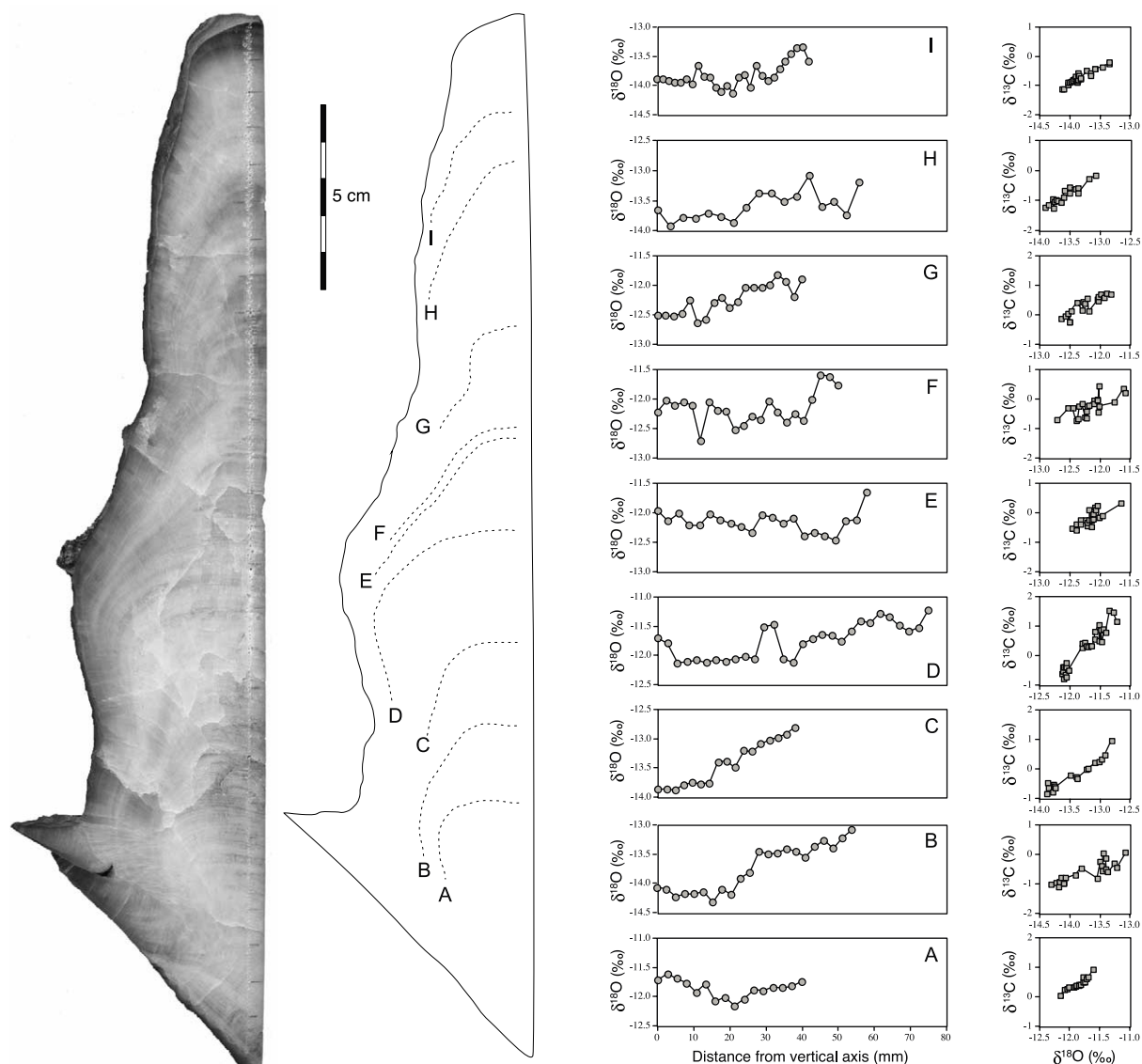Errors are quoted as 2-σ standard deviations.

Fig. 2. Polished slab of the left half of stalagmite SPA 49 showing its weakly laminated internal structure and the locations and results of nine 'Hendy tests', labeled A–I. Note slightly different range of stable isotope diagrams.

~36 μm/yr between 57.4 and ~50.4 kyr followed by a reduced growth rate of 8 μm/yr until ~46.3 kyr (Fig. 3).

The stable oxygen isotopic composition varies significantly along the extension axis. Initial calcite at 57 kyr shows $\delta^{18}O$ values of -12.9‰ which decrease to -14.0‰ (Fig. 4). $\delta^{18}O$ values rapidly increase between 55.6 and 55.3 kyr to values of -11.8‰ followed by a likewise rapid de-

crease. A short-lived event of high $\delta^{18}O$ values is recorded at 54.9 kyr. Between 54.3 and 54.1 kyr $\delta^{18}O$ values again increase by about 2‰ and stay near -11.8‰ for 3.0 kyr, followed by a gradual decline to low values of -14‰. The topmost calcite records an rapid increase in $\delta^{18}O$ starting at 47.0 kyr (Fig. 4).

Tests for isotopic equilibrium reveal a general tendency for $\delta^{18}O$ values to increase from the ax-
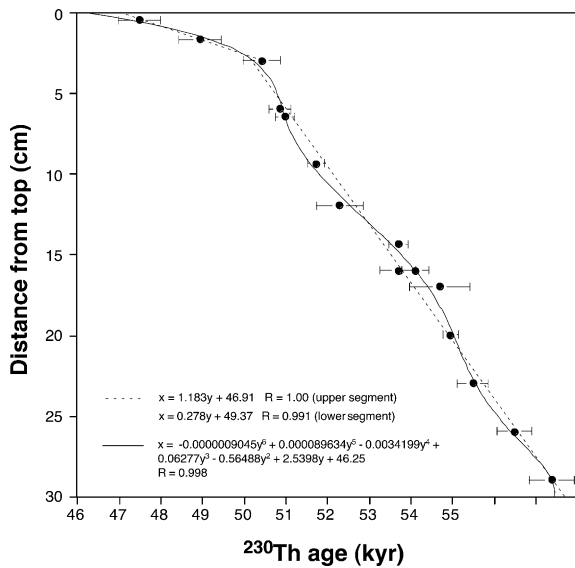
Fig. 3. Thickness-age model for stalagmite sample SPA 49. The error bars indicate 2-σ analytical uncertainties of TIMS ages. Shown are the preferred age model (solid line) vs. a two-step linear model (dashed line).

ial zone down the flank of the stalagmite (Fig. 2), although no clear-cut trend is apparent within 20 mm of the apex. The $\delta^{18}O$ values typically increase by up to 1‰ down the flank within a distance of ∼40–50 mm from the apex. C and O isotope values covary along individual growth laminae inasmuch as a 0.5‰ increase in $\delta^{18}O$ is accompanied by a ∼1.5‰ increase in $\delta^{13}C$ (Fig. 2).

4. Discussion

4.1. Th/U chronology

The TIMS dates indicate that stalagmite SPA 49 formed over ∼10 kyr during isotope stage 3, which, combined with our age model, suggests that the entire sample encompasses some 11 kyr. The lack of unconformities as shown by multiple Th/U samples as well as petrography suggests that calcite accreted continuously during this time interval. The stalagmite extension rate did not change significantly during most of the growth period except for the topmost part (after 50.4 kyr), when growth slowed down. Given the mod-

ern cave temperature of +2.3°C, the presence of calcite provides evidence that the mean annual air temperature at this altitude – which is known to correlate closely with the interior cave air temperature [24] – was within a couple of degrees of the present-day value. Had the temperature dropped well below this, permafrost would be expected to have formed above the cave thus greatly diminishing the supply of liquid water to the karst fissure network and stopping calcite deposition.

4.2. Stable isotope fractionation

The fidelity of calcite $\delta^{18}O$ values as a proxy of the paleoprecipitation-$\delta^{18}O$ depends heavily on the assumption that the latter has remained unaltered. This assumption is difficult to test. Replicating a record using one or more additional speleothem samples of the same tightly constrained Th/U chronology, but from different parts of the cave or from neighboring cave sites adds credibility, but not necessarily proof. Replicating the SPA 49 record is currently impossible given the scarcity of well developed stalagmites at this site.

Hendy [29] proposed a set of criteria to check for equilibrium versus kinetic fractionation within individual stalagmites. This 'Hendy test' requires a series of stable isotope analyses along individual growth layers from the apex (closest to the drip water source) laterally down the sides of the stalagmite, i.e. along the former flow path of the water film. At high drip rates, low pCO_2 gradients between karst aquifer and cave atmosphere, and relative humidity levels approaching condensation, the isotopic composition of calcite is largely independent of the distance from the apex. Conversely, long intervals between drops and aquifer-pCO_2 values much higher than those in the cave chamber will result in more extensive degassing of CO_2 along the water film path and a concomitant progressive increase in $\delta^{13}C$ due to Rayleigh-type distillation. A long residence time of the water film promotes mild evaporation even in caves where the relative humidity levels are high giving rise to an increase in $\delta^{18}O$ as the water slowly migrates down the sides.

Nine 'Hendy tests', more than performed by any previous speleothem study, show little change
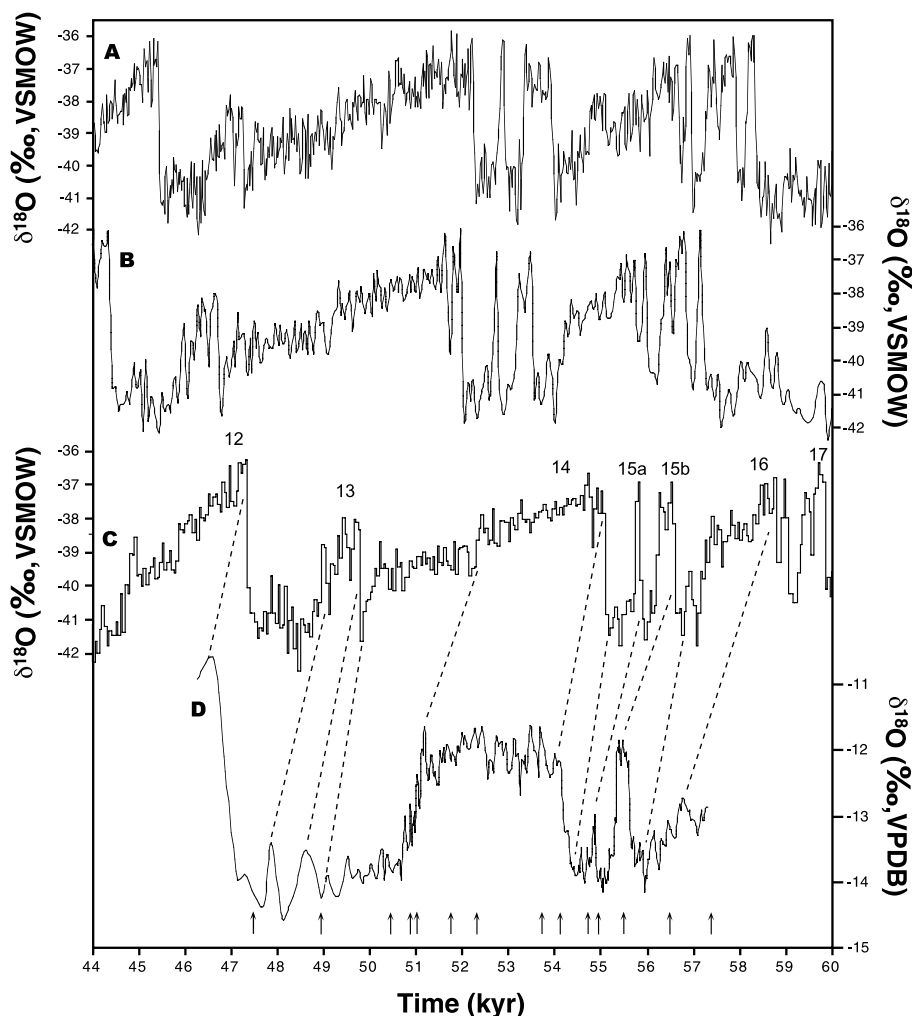
Fig. 4. Comparison of oxygen isotope records of the Greenland ice cores and stalagmite SPA 49. (A) GISP2 record [20,21]. (B) GRIP 1995 time scale [26]. (C) GRIP 2001 chronology [22]. (D) Stalagmite SPA 49. Numbers refer to Greenland Interstadials. Upward arrows indicate positions of TIMS samples. Dashed lines indicate major marker events used for cross-correlation.

in $\delta^{18}O$ within a radius of ~ 20 mm from the stalagmite's apex, followed by an increase in both $\delta^{18}O$ and $\delta^{13}C$ down the flanks (Fig. 2). This relationship is diagnostic of nonequilibrium fractionation in the more distal parts of the speleothem surface and implies a combination of strong degassing and concomitant slight evaporative enrichment along the flanks of the stalagmite. Some of the data points are significantly lower or higher than the neighboring samples within some of the isotope traces (Fig. 2). This variability is most likely due to the difficulty in precisely tracking individual growth laminae in this poorly laminated sample and is attributed to mixtures of adjacent growth laminae.

Speleothem samples that do not pass the equilibrium criteria set by the 'Hendy test' are commonly regarded as less useful in terms of paleoenvironmental reconstructions than those that do not show kinetic isotopic enrichment. While this is demonstrably true in many cases, we will make the case here that some of these samples – exemplified by SPA 49 – do in fact provide valuable information on long-term variations of the iso-

topic composition of the drip waters. We base our confidence on four lines of observations. First, lamina sampling shows that kinetic isotope fractionation does not occur within the axial zone but is restricted to the sides of the stalagmite. It is the axial zone that is being sampled for secular variations in stable isotopes which appears to be unaffected by kinetic fractionation (Fig. 2). Second, the 11-kyr $\delta^{18}O$ record of SPA 49 shows a well defined pattern of low and high values strongly resembling isotopic records reported from the Greenland ice cores (see below). Even the amplitudes of the $\delta^{18}O$ peaks show a consistent pattern arguing in favor of a largely unaltered isotopic signal. Note that the amplitude of these peaks is much larger than the variability that is present within individual laminae of the axial zone (2.5‰ vs. ≤ 0.5‰). Third, a comparison of this supposedly climatically controlled isotopic pattern and the multiple 'Hendy tests' shows no relationship. In other words, calcite deposited during times of apparently cold conditions (represented by 'Hendy tests' B, C, H, and I) shows the same general pattern of isotopic enrichment along the flanks as depicted by calcite formed under warm (interstadial) conditions ('Hendy tests' A, D, E, F, and G). Hence, the variation in the long-term oxygen isotopic signal is not controlled by kinetic fractionation. Lastly, slow drip rates and hence a higher potential for nonequilibrium isotope fractionation is expected during cold periods at this alpine site. Therefore, $\delta^{18}O$ values of calcite deposited during these periods – had they been controlled primarily by kinetic fractionation – should be biased toward high values, which is exactly the opposite of what is been observed (Fig. 2). As a consequence, we regard the isotope record obtained from the axial portion of SPA 49 as representative of the unaltered karst water signal.

4.3. Oxygen isotope record

The stable isotopic profile of sample SPA 49 shows long-term changes in $\delta^{18}O$ with superimposed high-frequency variations (Fig. 4). The most remarkable feature is the interval of consistently high $\delta^{18}O$ values after ∼54.3 kyr showing an abrupt start and a slightly more gradual return

to the initially low $\delta^{18}O$ values after 51.1 kyr. We interpret this prolonged interval as a major interstadial in the Alps, when the $\delta^{18}O$ value of meteoric precipitation increased rapidly due to warming of the atmosphere above the Central Alps. Concomitant warming of the cave interior will partially counteract this isotopic effect due to the temperature-dependent fractionation during calcite precipitation from aqueous solutions [25]. As a result, the actual increase of the meteoric $\delta^{18}O$ signal was larger than the measured ∼2‰, but the precise amount remains to be determined using independent methods (e.g. isotopic composition of fluid inclusions). It would be desirable to be able to calculate the degree of warming, but the relationship between air temperature and $\delta^{18}O$ of precipitation is not known for glacial climates, let alone secondary orographically induced isotopic shifts in mountainous regions such as the Central Alps. Nevertheless, the > 2‰ amplitude is substantial and clearly beyond that of isotopic changes of precipitation during the Holocene. The prominent ∼3000-yr long interstadial was preceded by two shorter warmings, a ∼300-yr interstadial centered at 55.4 kyr and a minor one 54.9 kyr ago (Fig. 4). The latter event clearly did not develop into a full interstadial and apparently lasted only some 100 yr.

4.4. Comparison with the ice cores

Comparison of the stable isotopic pattern of SPA 49 with the ice core records from central Greenland reveals a striking similarity (Fig. 4), inasmuch as the amplitude and structure of these warmings match GIS 15b and 14, as well as the small interstadial in between the two (Fig. 4), referred to as GIS 15a [7]. Equivalents of GIS 16 and 13 are also present albeit at smaller amplitude (Fig. 4). GIS 15b is characterized by an extremely rapid start and end in Greenland and lasted only ∼350 yr there. Its maximum is characterized by a bifurcation in the ice core, a feature also indicated in SPA 49. The same event lasted ∼300 yr in the Eastern Alps and reached the same $\delta^{18}O$ values as the following GIS 14 (−11.8‰), consistent with the isotopic curve from Greenland (Fig. 4). GIS

14 was the longest of the warm phases in Greenland during isotope stage 3 and its isotopic trace shows the characteristic D/O saw-tooth shape. The stalagmite record shows that this interstadial also started with a rapid warming in the Alps, but the air temperature then apparently remained warm for ∼3000 yr followed by a steep drop. In contrast, air temperature over central Greenland steadily decreased after the initial rapid warming (Fig. 4).

The absolute chronologies of the Greenland ice cores during isotope stage 3 are still rather inaccurate involving an uncertainty of up to ± 5–± 10% [16]. A recently proposed revised chronology for the GRIP ice core [22] – hereafter referred to as the GRIP 2001 chronology – results in significantly older ages, e.g. the onset of GIS 14 is

placed at 55.1 kyr as compared to 52.0 kyr in the previous GRIP 1995 and GISP2 time scales [21,26]. Our new Th/U dated chronology of SPA 49 suggests that the start of GIS 14 occurred in between these proposed dates, but closer to the GRIP 2001 chronology, i.e. at 54.2 kyr (Fig. 4). Moreover, GIS 15b started 55.6 kyr ago in the Alps, which is some 1000 yr later than the GRIP 2001 chronology suggests, but some 2100 yr earlier than the GRIP 1995 chronology.

Correlation with the Greenland ice cores becomes less clear in the uppermost part of sample SPA 49 which is primarily due to the reduced growth rate (Fig. 3). The ice cores show a gradual decline of O isotope values during GIS 14 separated by a step-like feature in the middle of GIS 14 and followed by a short-lived GIS (No. 13).
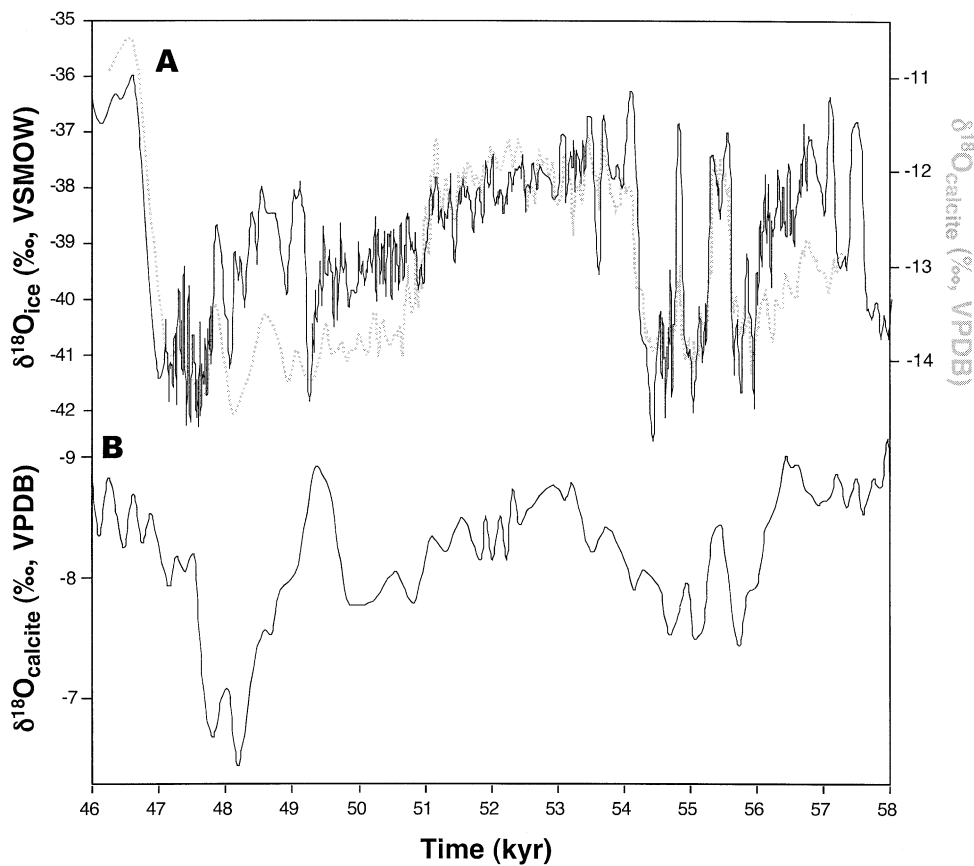

Fig. 5. (A) GRIP O isotope record tuned according to the Th/U dated stalagmite record from Kleegruben Cave. Relevant common features in the two O isotope records were used as tie points (see Fig. 4) and tuning was performed using AnalySeries 1.1 [27]. R = 0.76. (B) Stalagmite sample MSL of Hulu Cave in eastern China [23] (note reverse isotope scale).

SPA 49 reveals stable climatic conditions during GIS 14 with a minor peak at the end followed by a rather steep decline to stadial O isotopic compositions (Fig. 4). A small equivalent of GIS 13 is present in this record, and the very top shows a rapid increase of the O isotopic composition which correlates nicely with the rapid onset of GIS 12 in the Greenland ice cores (GRIP 2001 chronology).

The precise chronology of SPA 49 offers the opportunity to tune the O isotope record of the Greenland ice cores to the stalagmite (Fig. 5), whereby characteristic features of both O isotope records (Fig. 4) are used as tie points. This results in a highly significant correlation (R = 0.76). The new age model is in good agreement with the GRIP 2001 chronology but suggests a somewhat shorter duration of GIS 14 (1.8 vs. 2.5 kyr in [22]). According to the new chronology, GIS 14 commenced at 54.2 and ended at 51.0 ka (Fig. 5).

4.5. Comparison with other records

Currently available records from the European continent lack the necessary precision to allow direct comparison with SPA 49. It is interesting to note, however, that a detailed pollen record from the lacustrine section at Lago Grande di Monticchio in southern Italy reveals a series of high-frequency warmings attributed to D/O cycles [13]. The longest of these warming phases (pollen zone 11) had an estimated duration of 6.4 kyr and was correlated to GIS 14 [15], although the proposed age model suggested somewhat lower ages. Provided that this correlation hold true, GIS 14 could have been indeed the longest D/O warm phase in Europe during isotope stage 3, although our data indicate that this interstadial lasted significantly shorter than suggested by [15].

New data from Th/U dated coral terraces in the SW Pacific underscore the warm notion of peak isotope stage 3 global climate and provide a strong case for a sea level only 30–60 m below present level 45–50 kyr ago [28].

Recently, two stalagmite records from the monsoon region of eastern China became available the O isotopic profiles of which show similarities to Greenland D/O events [23]. One of these speleo-

thems covers the time interval of sample SPA 49 and shows close similarities to our stable isotope record, such as possible equivalents of GIS 15a and 15b (Fig. 5). Their timing, constrained by Th/U TIMS analyses, is in good agreement with our record. It is encouraging to see this fit of the three isotope records obtained from completely different environments in the Northern Hemisphere. Differences in the timing of GIS 13 and the onset of GIS 12 are attributed to the less accurate chronology in the upper portion of SPA 49. Also note that isotope excursions in the Hulu Cave record are in the opposite direction as compared to the records from Greenland and the Alps. This behavior has been attributed to the 'amount effect' that dominates the stable isotope composition of precipitation in monsoonal settings [23].

4.6. Implications and conclusions

Stalagmite SPA 49 preserves a unique isotopic record of rapid climate change in the European Alps, tightly constrained by Th/U dates. Despite the fact that the outer portions of individual growth laminae depict evidence of kinetically controlled isotope fractionation, several lines of observations indicate that calcite precipitation near the apex of the stalagmite occurred under near-equilibrium conditions thus validating the paleoenvironmental significance of this exceptional record. Located in an environmentally sensitive, high-alpine (2165 m a.s.l.) cave, the mere presence of speleothem calcite demonstrates that at this altitude mean air temperatures stayed within a few degrees of the present-day one during D/O events. We emphasize that there is no petrographic, stable isotopic nor Th/U chronological evidence of hiatuses during stadials. Given the close atmospheric connections between Greenland and central Europe, it seems justified to directly compare interstadials in both regions, particularly since both records are based on the same proxy, stable oxygen isotopes of precipitation. Our data suggest that rapid climate warmings associated with GIS 15 and 14 occurred 55.6 and 54.2 kyr ago, significantly earlier than suggested by the GRIP 1995 and GISP2 time scales, but only

slightly later than indicated by the GRIP 2001 chronology [22]. In addition, the SPA 49 record indicates that the warm conditions during GIS 14 lasted only 3000 yr in the Alps as opposed a significantly long duration (5000 yr) suggested by the ice cores.

Acknowledgements

References

[1] S.J. Johnsen, H.B. Clausen, W. Dansgaard, K. Fuhrer, N. Gundestrup, C.U. Hammer, P. Iversen, J. Jouzel, B. Stauffer, J.P. Steffensen, Irregular glacial interstadials recorded in a new Greenland ice core, Nature 359 (1992) 311–313.

[2] W. Dansgaard, S.J. Johnsen, H.B. Clausen, D. Dahl-Jensen, N.S. Gundestrup, C.U. Hammer, C.S. Hvidberg, J.P. Steffensen, A.E. Sveinbjörnsdottir, J. Jouzel, G. Bond, Evidence for general instability of past climate from a 250-kyr ice-core record, Nature 364 (1993) 218–220.

[3] C. Lang, M. Leuenberger, J. Schwander, S. Johnsen, 16°C rapid temperature variation in central Greenland 70,000 years ago, Science 286 (1999) 934–937.

[4] J. Jouzel, Calibrating the isotopic paleothermometer, Science 286 (1999) 910–911.

[5] G. Bond, W. Broecker, S. Johnsen, J. McManus, L. Labeyrie, J. Jouzel, G. Bonani, Correlations between climate records from North Atlantic sediments and Greenland ice, Nature 365 (1993) 143–147.

[6] G.C. Bond, W. Showers, M. Elliot, M. Evans, R. Lotti, I. Hajdas, G. Bonani, S. Johnson, The North Atlantic's 1–2 kyr climate rhythm: Relation to Heinrich events, Dansgaard/Oeschger cycles and the Little Ice Age, in: P.U. Clark, R.S. Webb, L.D. Keigwin (Eds.), Mechanisms of Global Climate Change at Millennial Time Scales, Geophysical Monograph 112, 1999, pp. 35–58.

[7] S. van Kreveld, M. Sarnthein, H. Erlenkeuser, P. Grootes, S. Jung, M.J. Nadeau, U. Pflaumann, A. Voelker, Potential links between surging ice sheets, circulation changes, and the Dansgaard–Oeschger cycles in the Irminger Sea, 60–18 kyr, Paleoceanography 15 (1999) 425–442.

[8] N.J. Shackleton, M.A. Hall, E. Vincent, Phase relationships between millennial-scale events 64,000–24,000 years ago, Paleoceanography 15 (2000) 565–569.

[9] I.L. Hendy, J.P. Kennett, Dansgaard–Oeschger cycles and the California Current System: Planktonic foraminiferal response to rapid climate change in Santa Barbara Basin, Ocean Drilling Program hole 893A, Paleoceanography 288 (2000) 30–42.

[10] J.P. Sachs, S.J. Lehman, Subtropical North Atlantic temperatures 60,000 to 30,000 years ago, Science 286 (1999) 756–759.

[11] H. Schulz, U.v. Rad, H. Erlenkeuser, Correlation between Arabian Sea and Greenland climate oscillations of the past 110,000 years, Nature 393 (1998) 54–57.

[12] T. Blunier, E.J. Brook, Timing of millennial-scale climate change in Antarctica and Greenland during the last glacial period, Science 291 (2001) 109–112.

[13] J.R.M. Allen, U. Brandt, A. Brauer, H.W. Hubberten, B. Huntley, J. Keller, M. Kraml, A. Mackensen, J. Mingram, J.F.W. Negendank, N.R. Nowaczyk, H. Oberhänsli, W.A. Watts, S. Wulf, B. Zolitschka, Rapid environmental changes in southern Europe during the last glacial period, Nature 400 (1999) 740–743.

[14] M. Follieri, M. Giardini, D. Magri, L. Sadori, Palynostratigraphy of the last glacial period in the volcanic region of Central Italy, Quat. Int. 47 (1998) 3–20.

[15] W.A. Watts, J.R.M. Allen, B. Huntley, Palaeoecology of three interstadial events during oxygen-isotope Stages 3 and 4: A lacustrine record from Lago Grande di Monicchio, southern Italy, Palaeogeogr. Palaeoclimatol. Palaeoecol. 155 (2000) 88–93.

[16] D.A. Meese, A.J. Gow, R.B. Alley, G.A. Zielinski, P. Grootes, M. Ram, K.C. Taylor, P.A. Mayewski, J.F. Bolzan, The Greenland Ice Sheet Project 2 depth-age scale methods and results, J. Geophys. Res. 102/C12 (1997) 26411–26423.

[17] C. Spötl, S.J. Burns, N. Frank, A. Mangini, A., R. Pavuza, Speleothems from the High-Alpine Spannagel Cave, Zillertal Alps (Austria), in: I.D. Sasowsky, J. Mylroie (Eds.), Studies of Cave Sediments, Kluwer, Dordrecht, in press.

[18] H. Cheng, R.L. Edwards, J. Hoff, C.D. Gallup, D.A. Richards, Y. Asmerom, The half-lives of uranium-234 and thorium-230, Chem. Geol. 169 (2000) 17–33.

[19] N. Frank, M. Braum, U. Hambach, A. Mangini, G. Wagner, Warm period growth of travertine during the Last Interglaciation in southern Germany, Quat. Res. 54 (2000) 38–48.

[20] P.M. Grootes, M. Stuiver, J.W.C. White, S. Johnsen, J. J. Jouzel, Comparison of oxygen isotope records from the GISP2 and GRIP Greenland ice cores, Nature 366 (1993) 552–554.

[21] M. Stuiver, P.M. Grootes, T.F. Braziunas, The GISP2 delta 18O climate record of the past 16,500 years and the role of the sun, ocean, and volcanoes, Quat. Res. 44 (1995) 341–354.

[22] S.J. Johnsen, D. Dahl-Jensen, N. Gundestrup, J.P. Stef-

fensen, H.B. Clausen, H. Miller, V. Masson-Delmotte, A.E. Sveinbjörnsdottir, J. White, Oxygen isotope and palaeotemperature records from six Greenland ice-core stations: Camp Century, Dye-3, GRIP, GISP2, Renland and NorthGRIP, J. Quat. Sci. 16 (2001) 299–307.

[23] Y.J. Wang, H. Cheng, R.L. Edwards, Z.S. An, J.Y. Wu, C.C. Shen, J.A. Dorale, A high-resolution absolute-dated late Pleistocene monsoon record from Hulu Cave, China, Science 294 (2001) 2345–2348.

[24] T.M.L. Wigley, M.C. Brown, The physics of caves, in: T.D. Ford, C.H.D. Cullingford (Eds.), The Science of Speleology, Academic Press, London, 1976, pp. 329–358.

[25] I. Friedman, J.R., O'Neil, Compilation of stable isotope fractionation factors of geochemical interest, in: M. Fleischer (Ed.), Data of Geochemistry, 6th edn., U.S. Geol. Survey Prof. Paper 440-KK, 1977, pp. 1–12.

[26] S.J. Johnsen, D. Dahl-Jensen, W. Dansgaard, N. Gundestrup, Greenland palaeotemperatures derived from GRIP bore hole temperature and ice core isotope profile, Tellus 47B (1995) 624–629.

[27] D. Paillard, L. Labeyrie, P. Yiou, Macintosh Program Performs Time-Series Analysis, Eos, Trans. Am. Geophys. Union 77, p. 379 (http://www.agu.org/eos_elec/96097e.html).

[28] G. Cabioch, L.K. Ayliffe, Raised coral terraces at Malakula, Vanuatu, Southwest Pacific, indicate high sea level during marine isotope stage 3, Quat. Res. 56 (2001), pp. 357-365.

[29] C.H. Hendy, The isotopic geochemistry of speleothems-I. The calculation of the effects of different modes of formation on the isotopic composition of speleothems and their applicability as palaeoclimatic indicators, Geochim. Cosmochim. Acta 35 (1971) 801–824.